Soft Matter

Volume 1 | Number 1 | Jan 2013 | Pages 1–100

Soft Matter

www.rsc.org/softmatter

ROYAL SOCIETY OF CHEMISTRY

www.rsc.org/softmatter

The wetting transitions from complete to partial wetting and to complete dewetting are identified within a membrane compartment. The dependences of wetting transitions on material parameters, such as the intrinsic contact angles, the interaction strengths between the polymers and between the membrane and polymer η_p, and impermeability of the membrane to the enclosed polymers, are investigated.
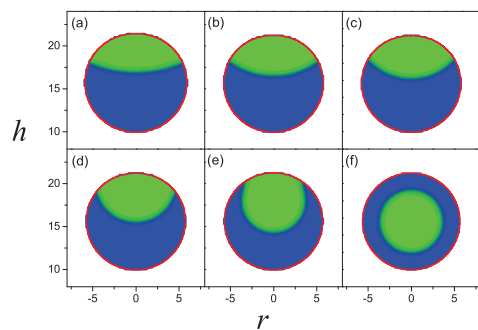
Wetting transitions within membrane compartments

Kunkun Guo,[1] Wenjia Xiao,[1] and Kenichi Yoshikawa[2]

[1] *College of Materials Science and Engineering, Hunan University, Changsha, 410082, China*
[2] *Department of Physics, Graduate School of Science, Kyoto University, Kyoto 606-8502, Japan*
(Dated: May 15, 2014)

A biomimetic membrane in contact with several aqueous phases is theoretically studied using a combination of Helfrich curvature elasticity theory for fluid membranes and self-consistent field theory for polymers in solutions. Two phases that are thermodynamically formed by phase separation of aqueous solutions, as well as stable and metastable shapes of fluid vesicles, have been observed. The wetting transitions from complete to partial wetting and to complete dewetting are identified within a membrane compartment. The dependences of wetting transitions on material parameters, such as the intrinsic contact angles θ_{in}, the interaction strengths between the polymers $\chi_{\alpha\beta}$ and between the membrane and polymer η_p, and impermeability of the membrane to the enclosed polymers ζ_p, are investigated. For a given $\chi_{\alpha\beta}$, impermeability ζ_p and affinity to membrane η_p, θ_{in} is found to be a constant and independent of the reduced volume of vesicles and the volume fraction of two phases.

I. INTRODUCTION

Liquid droplets on flat surfaces may exhibit the contact angle in the range from 0 to 180^0, and the wetting transitions from complete to partial wetting and to complete dewetting correspond to a certain change in contact angles[1,2]. Such transitions have been intensively studied for fluid-fluid interfaces in binary mixtures, for liquid droplets at solid substrates and at chemically patterned or topographically structured substrates[1–3]. However, the wetting transitions within a mesoscopic membrane compartment are more fascinating due to the relevance to the force balance along three bending interfaces[4–6].

The cytoplasm of living cells is a complex fluid exhibiting spatial self-organization on different scales[7]. A range of biological processes are realized by the spatially-dependent phase separation of cytoplasmic components[8]. Recently, lipid vesicles/droplets and two species of polymers such as dextran/DNA and polyethylene glycol (PEG), have attracted wide attention experimentally as model cellular systems because of their relevance to aqueous-aqueous phase separation and shape transformations of vesicles[5,6,9–12]. Phase separation within the vesicles can be induced by changing osmotic conditions or temperatures. Due to the impermeability of the membrane to the encapsulated polymers and the permeability of the membrane to water molecules, a volume of the vesicles is reduced and two phases would be formed. Interesting phenomena relevant to the phase separation processing, such as partial to complete wetting transitions of aqueous phases within membrane compartments[5,6], vesicle budding and fission[10,11], and membrane tube formation[12], are experimentally observed, but remain poorly understood.

A mesoscopic theory for vesicles encapsulating two aqueous phases has been developed that starts from the simple observation of the vesicle state in contact with two phases in experiments[13]. A material parameter, the intrinsic contact angle, θ_{in}, has been revealed between the membrane and aqueous phases. They found that the angle θ_{in} is a constant and independent of the reduced volume of vesicles. However, the wetting transitions of aqueous phases, as well as the dependence of wetting transitions and material parameters, are still unresolved beyond the theory.
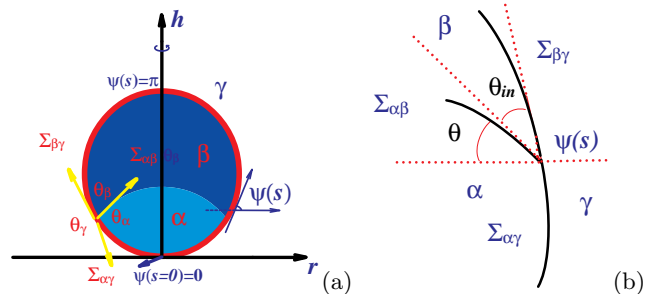

FIG. 1. (color online) (a) A schematic illustration of an axisymmetric vesicle encapsulating two aqueous phases α and β indicated by two colors. The γ phase indicates solutions outside of the vesicle. The vesicle shape along the contact line can be characterized by three effective contact angles θ_α, θ_β, and θ_γ with $\theta_\alpha + \theta_\beta + \theta_\gamma = 2\pi$, and these contact angles are related to the three tensions $\Sigma_{\alpha\beta}$, $\Sigma_{\alpha\gamma}$, and $\Sigma_{\beta\gamma}$. s denotes the arc-length along the contour measured from the south pole of the shape. $\psi(s)$ is the angle between the tangent to the contour and the r axis: $r = 0$, $\psi(0) = 0$ at the south pole, where $r = 0$, $\psi(s) = \pi$ at the north pole. (b) Enlarged view close to the contact line: Intrinsic contact angle θ_{in} between two planes that are tangential to the $\alpha\beta$ interface and the smoothly curved vesicle membrane, respectively. The tangent angle θ is between the plane tangential to the $\alpha\beta$ interface and horizontal plane.

We have developed the microscopic theoretical framework by combining the Helfrich curvature theory for vesicle membranes and self-consistent field theory for polymers. This has been used to explore the polymer anchoring vesicle system[14–16], and extended to study vesicles in contact with two aqueous phases[17]. Both stable and metastable vesicle shapes including prolates, oblates and stomatocytes, and spatial distributions of two phases α

and β have been achieved[17]. From phase behaviors of a wide variety of vesicles encapsulating two aqueous phases, we find that the effective contact angle along the three contact lines exhibits a certain change, and the wetting transitions are also observed within membrane compartments. As a result, the effective contact angle and intrinsic contact angle are determined from mechanical equilibrium, and the dependence of wetting transitions on material parameters are investigated.

II. MODEL

The vesicle containing two aqueous phases in an axisymmetric coordinate system is shown schematically in Fig. 1. Two aqueous phases are formed by n_α Gaussian polymer chains α with N_α segments and n_β Gaussian polymer chains β with N_β segments dissolved in n_{so} solvent molecules distributed in the interior of the vesicle membrane. The lipid membrane provides a semipermeable, flexible boundary around polymers. In general, the solvent molecules can freely permeate through the membrane, but chain segments can not. In experiments[12,13], osmotically balanced vesicles are obtained after waiting 21 hours, at which time each phase is homogeneous. Therefore, we assume homogeneous phases together with incommensurability at the reference density $\rho_0 \propto 1/b^3$, where b is equal to the Kuhn statistic lengths of the polymer chains α and β, the size of the a single solvent molecule, and the lateral unit length of the vesicle membrane. In general, the thickness of a lipid bilayer is about 5 nm, thus $b \simeq 5$ nm. The partition function of such a system is given by

$$\Xi \propto \frac{1}{n_\alpha! n_\beta! n_{so}!} \int \prod_{i=1}^{i=n_{so}} D\mathbf{R}_{so}^i \int D\mathbf{R}_m \exp\{-H_m^0[\mathbf{R}_m]\} \quad (1)$$

$$\prod_{p=\alpha,\beta} \int \prod_{i=1}^{i=n_p} D\mathbf{R}_p^i(\tau) \exp\{-H_p^0[\mathbf{R}_p^i(\tau)]\} \exp\{-H_{int}\}$$

$$\prod_\mathbf{r} \delta[1 - \hat{\phi}_{so}(\mathbf{r}) - \sum_{p=\alpha,\beta} \hat{\phi}_p(\mathbf{r})]\delta[\int_{\mathbf{r} \ni V[\mathbf{R}_m]} d\mathbf{r} \sum_{p=\alpha,\beta} \hat{\phi}_p(\mathbf{r})]$$

where $\int D\mathbf{R}$ denotes the path integral over all possible conformations of chain segments, membrane and solvent molecules. $\mathbf{R}_{so}^i$ and $\mathbf{R}_p^i(\tau)$ represent spatial positions of the solvent i and the segment τ of the ith polymer chains, respectively. $\mathbf{R}_m$ is the spatial position of a vesicle. $\mathbf{r} \in V[\mathbf{R}_m]$ and $\mathbf{r} \ni V[\mathbf{R}_m]$ mean that the spatial positions are located in the interior and exterior of the vesicle, respectively. In addition, the first Dirac function is introduced to impose the incompressibility constraint, and the second Dirac function ensures that polymer chains p remain in the interior of the vesicle. The script (p) takes the two values α and β, indicating the two different types of polymer chains. The density operators are defined as $\hat{\phi}_p(\mathbf{r}) = 1/\rho_0 \sum_{i=1}^{n_p} \int_0^{N_p} d\tau \delta[\mathbf{r} - \mathbf{R}_p^i(\tau)]$ and $\hat{\phi}_{so}(\mathbf{r}) = 1/\rho_0 \sum_{i=1}^{n_{so}} \delta[\mathbf{r} - \mathbf{R}_{so}^i]$. Under the condition that

solvent molecules can freely penetrate the membrane, the interactions between the membrane and solvent can be neglected. Therefore, the interaction Hamiltonian, H_{int}, includes the polymer-solvent molecules (V_{ps}), polymer α-polymer β ($V_{\alpha\beta}$) and polymer-membrane (V_{pm}) interactions, i. e. $H_{int} = V_{ps} + V_{\alpha\beta} + V_{pm}$. They are $\hat{V}_{\alpha\beta} = \chi_{\alpha\beta}\rho_0 \int d\mathbf{r}\hat{\phi}_\alpha(\mathbf{r})\hat{\phi}_\beta(\mathbf{r})$, $\hat{V}_{ps} = \chi_{ps}\rho_0 \int d\mathbf{r}\hat{\phi}_p(\mathbf{r})\hat{\phi}_{so}(\mathbf{r})$ and $\hat{V}_{pm} = \eta_{pm}b\rho_0 \oint dA\hat{\phi}_p[\mathbf{r} = \mathbf{R}_m]$, where $\chi_{\alpha\beta}$, χ_{ps} and η_{pm} are Flory-Huggins interaction parameters of polymer (α)-polymer (β), polymer-solvent and polymer-membrane pairs, respectively.

The Hamiltonian of the Gaussian polymer chain has been formulated as

$$H_p^0[\mathbf{R}_p] = 3/2b^2 \int_0^{N_p} d\tau[d\mathbf{R}_p(\tau)/d\tau]^2. \quad (2)$$

The Hamiltonian of the membrane[18,19] has the form

$$H_m^0[\mathbf{R}_m] = \kappa/2 \oint_{A=\mathbf{R}_m} dA[2H + c_0]^2 + \lambda \oint_{A=\mathbf{R}_m} dA$$
$$+ \Delta P \int_{\mathbf{r} \in V[\mathbf{R}_m]} d\mathbf{r} \quad (3)$$

where κ, c_0 and H are the bending rigidity modules, spontaneous curvature and curvature of the fluid membrane, respectively. For a bilayer membrane containing two leaflets with an identical composition, $c_0 = 0$, and we focus on this case in this work. The tensile stress λ acting on the membrane and the pressure difference $\Delta P = p_{out} - p_{in}$ across the membrane are Lagrange multipliers of the vesicle surface area A and vesicle volume V, respectively.

Performing Hubbard-Stratonovich transformations[20], the Lagrange multiplier ξ is introduced to ensure the incompressible constraint of the system and one material parameter ζ_p is introduced to express the impermeability of the membrane to the polymer, which is opposite to the permeability coefficient of membrane to polymer as measured by experiments. The external auxiliary fields $\omega_p(\mathbf{r})$ and $\omega_{so}(\mathbf{r})$ are self consistent molecular fields conjugated to local volume fractions $\phi_p(\mathbf{r})$ and $\phi_{so}(\mathbf{r})$, respectively. The partition function can be expressed as a function integral of the density and external fields

$$\Xi \propto \int D\mathbf{R}_m \int D\phi_{so} \int D\omega_{so} \int D\xi \prod_{p=\alpha,\beta} \int D\phi_p \quad (4)$$
$$\int D\omega_p \int D\zeta_p \exp\{-F[\phi_p, \omega_p, \zeta_p, \phi_{so}, \omega_{so}, \xi, \mathbf{R}_m]\}$$

where the free energy functional F is defined as

$$F\left[\phi_p, \omega_p, \zeta_p, \phi_{\text{so}}, \omega_{\text{so}}, \xi, \mathbf{R}_m\right] \qquad (5)$$

$$= \chi_{\alpha\beta} \int d\mathbf{r} \phi_\alpha \phi_\beta + \sum_{p=\alpha,\beta} \chi_{ps} \int d\mathbf{r} \phi_p \phi_{\text{so}} - \int d\mathbf{r} \omega_{\text{so}} \phi_{\text{so}}$$

$$- \sum_{p=\alpha,\beta} \int d\mathbf{r} \omega_p \phi_p + \sum_{p=\alpha,\beta} \eta_{pm} b \oint_{A=\mathbf{R}_m} dA \phi_p$$

$$- n_{\text{so}} \ln Q_{\text{so}}(\omega_{\text{so}}) - \sum_{p=\alpha,\beta} n_p \ln Q_p(\omega_p) + \lambda \oint_{A=\mathbf{R}_m} dA$$

$$- \int d\mathbf{r} \xi [1 - \sum_{p=\alpha,\beta} \phi_p - \phi_{\text{so}}] + \sum_{p=\alpha,\beta} \zeta_p \int_{\mathbf{r} \ni V[\mathbf{R}_m]} d\mathbf{r} \phi_p$$

$$+ \frac{1}{2} \oint_{A=\mathbf{R}_m} [2H + c_0]^2 dA + \Delta P \int_{\mathbf{r} \in V[\mathbf{R}_m]} d\mathbf{r}$$

In Eqn. (5), the partition function of a single polymer chain $Q_p(\omega_p)$ and solvent molecules $Q_{\text{so}}(\omega_{\text{so}})$ under the potential fields, ω_p and ω_{so}, are $Q_{\text{so}}(\omega_{\text{so}}) = \int d\mathbf{r} e^{-\omega_{\text{so}}}$ and $Q_p(\omega_p) = \int d\mathbf{r} q_p(\mathbf{r}, \tau) q_p(\mathbf{r}, N_p - \tau)$, respectively. The τth segment distribution function $q_p(\mathbf{r}, \tau)$ obeys the modified diffusion equation

$$\frac{\partial}{\partial \tau} q_p(\mathbf{r}, \tau) = \frac{b^2}{6} \nabla^2 q_p(\mathbf{r}, \tau) - \omega_p(\mathbf{r}) q_p(\mathbf{r}, \tau) \qquad (6)$$

which is subject to the initial condition $q_p(\mathbf{r} \in V[\mathbf{R}_m], 0) = 1$.

By the mean-field approximation, the free energy in Eqn (5) is minimized with respect to ϕ_p, ϕ_{so}, ω_p, ω_{so}, ξ and ζ_p, respectively, obtaining a stable or metastable state of the system and yielding the self-consistent equations for polymers and solvents as follows,

$$\omega_\alpha = \begin{cases} \zeta_\alpha + \chi_{\alpha\beta}\phi_\beta + \chi_{\alpha s}\phi_s + \xi & \mathbf{r} \ni V[\mathbf{R}_m] \\ \eta_{\alpha m} + \chi_{\alpha\beta}\phi_\beta + \chi_{\alpha s}\phi_s + \xi & \mathbf{r} = \mathbf{R}_m \\ \chi_{\alpha\beta}\phi_\beta + \chi_{\alpha s}\phi_s + \xi & \mathbf{r} \in V[\mathbf{R}_m] \end{cases}, \quad (7)$$

$$\omega_\beta = \begin{cases} \zeta_\beta + \chi_{\alpha\beta}\phi_\alpha + \chi_{\beta s}\phi_s + \xi & \mathbf{r} \ni V[\mathbf{R}_m] \\ \eta_{\beta m} + \chi_{\alpha\beta}\phi_\alpha + \chi_{\beta s}\phi_s + \xi & \mathbf{r} = \mathbf{R}_m \\ \chi_{\alpha\beta}\phi_\alpha + \chi_{\beta s}\phi_s + \xi & \mathbf{r} \in V[\mathbf{R}_m] \end{cases}, \quad (8)$$

$$\omega_s = \sum_p \chi_{ps} \phi_p + \xi \qquad (9)$$

$$\phi_p = \frac{\overline{\phi}_p V}{Q_p} \int_0^{N_p} d\tau q_p(\mathbf{r}, \tau) q_p(\mathbf{r}, N_p - \tau) \qquad (10)$$

$$\phi_{\text{so}} = \frac{\overline{\phi}_s V}{Q_s} \exp[-\omega_{\text{so}}] \qquad (11)$$

$$1 = \sum_p \phi_p + \phi_{\text{so}} \qquad (12)$$

$$\int_{\mathbf{r} \ni V[\mathbf{R}_m]} d\mathbf{r} \phi_p = 0 \qquad (13)$$

According to the variational algorithms given in Refs.[15,16,18,19], the further minimization of the free energy F is performed with respect to the membrane. The derived shape equation of one vesicle in contact with two aqueous phases is

$$\sum_{p=\alpha,\beta} \{\eta_{pm} b[\mathbf{n} \cdot \nabla \phi_p(\mathbf{r} = \mathbf{R}_m)] - \zeta_p \phi_p(\mathbf{r} = \mathbf{R}_m)\}$$

$$+ \Delta P - 2H[\sum_{p=\alpha,\beta} \eta_{pm} b \phi_p(\mathbf{r} = \mathbf{R}_m) + \lambda]$$

$$+ \kappa(2H + c_0)(2H^2 - c_0 H - 2K) + 2\kappa \nabla^2 H = 0 \quad (14)$$

where K is the Gaussian curvature of the membrane, which is neglected due to the Gauss-Bonnet theorem[19], and the term $\mathbf{n} \cdot \nabla \phi_p(\mathbf{r} = \mathbf{R}_m)$ denotes the concentration gradient along the direction normal to the vesicle membrane.

The numerical scheme we use is similar to our previous studies[15–17]. This scheme begins with an initial assumption of a spherical vesicle shape, and then the self-consistent equations (6)-(13) are solved to obtain $\phi_p(\mathbf{r})$ and $\phi_{\text{so}}(\mathbf{r})$. The obtained $\phi_p(\mathbf{r})$ is then inserted into Eq. (14) to calculate the new shape of the vesicle. The steps are finished until the convergence conditions have been reached between two successive iterations. For a given tension λ and pressure difference ΔP, the convergence conditions are that the differences for both $d\psi(s)/ds$ and $\phi_p(r, h)$ between two successive iterations are less than 10^{-4}. In order to solve Eqs. (6)-(13), we set $N_\alpha = N_\beta = 100$, $b = 1$, $\Delta\tau = 1$, $\Delta r = \Delta h = 0.1\sqrt{N}b$, with the box size $L_r = 10$ and $L_h = 40$. Due to the impermeability of the membrane to the chain segments, the polymer chains are always located in the interior of the vesicle, and the polymer densities should therefore be altered together with shape transformations of vesicles. To simply describe the shape transformations of vesicles, the reduced volume v is introduced to obey with $v \equiv V/[(4\pi/3)(A/4\pi)^{3/2}]$, where V and A are the volume and surface of the vesicle. With decreasing reduced volume v, the biconcave character of a isolate vesicle becomes more pronounced, giving that $v = 1$ is for spherical object, v in the range of $0.65 \sim 1.0$ has an approximately prolate ellipsoidal shape and $v = 0.6$ corresponds to the normal human erythrocyte[19,21]. It is noted that the total polymer density encapsulated within a spherical vesicle ($v = 1$) is initially chosen. Phase separation with the vesicles can be induced by changing osmotic conditions in the experiments, water is released from vesicles during deflations, and then both the volume and apparent area of the vesicles would be reduced[5], Therefore, the vesicles after shape transformations generally contain almost the same number of chain segments with the original spherical vesicle that has the same surface area. Likewise, after equilibrium, both the α and β phases arrive at mechanical equilibrium with almost the same particle number

density of osmotically active particles. As a result, the resulting polymer densities ϕ_α and ϕ_β that are dependent on the shape transformation of the vesicle, could be determined, and the detailed procedure has been presented in Ref. 17.

III. RESULTS AND DISCUSSIONS

For the characteristics of the membrane/polymer systems studied here, the encapsulated polymer concentration is about 5 %, and the bending rigidity and interface tension of the membrane are $\kappa \simeq 10^{-19}$ J and on the order of 10 μN/m, respectively, which implies $R \simeq 100$ nm. As mentioned in the Section II, $b \simeq 5$ nm, the vesicles we calculated have the physical magnitude of diameter close to 100 nm. We choose the bending rigidity κ value to be 1-25 $k_B T$, as well as λ to be about 10^{-3} $k_B T/nm^2$, where T is a physiological temperature. The values of κ and λ, the size of the lipid vesicle, and the weight percentage of polymers are all comparable to the values observed experiments[5,12,22,23]. In the experiments[24,25], the permeability coefficients with respect to lipids are measured in the range from 136×10^{15} mol dyne^{-1} sec^{-1} for water to 0.9×10^{15} mol dyne^{-1} sec^{-1} for 1,4-butanediol, and the range of the permeability coefficient for oligomers is about one order of magnitude. The impermeability of polymer to membrane ζ_p, is about one order of magnitude and ranges from 1 to 10 $k_B T$, and the adsorption strength represented by η ranges from 0 to -0.1 $k_B T$, which are available from real experiments.
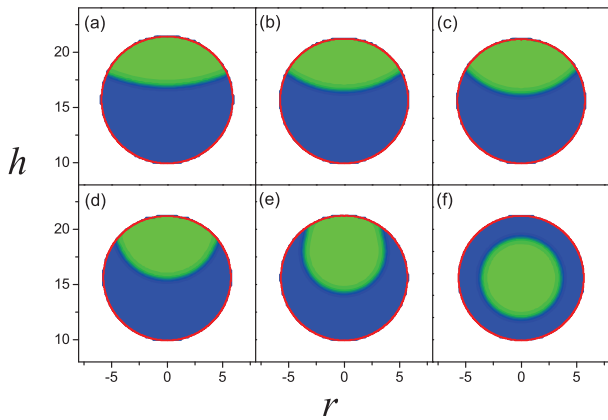

FIG. 2. (color online) Phases of vesicles encapsulating phase α (green) and phase β (blue) with $\phi_\alpha/\phi_\beta = 0.3/0.7$, $c_0 = 0$, $v \approx 1$, $\chi_{\alpha\beta} = 0.035$ at $\Delta\zeta = 0.4$ (a), $\Delta\zeta = 2.0$ (b), $\Delta\zeta = 3.6$ (c), $\Delta\zeta = 5.2$ (d), $\Delta\zeta = 6.8$ (e), $\Delta\zeta = 8.4$ (f).

Figure 2 presents the morphologies of a spherical vesicle containing two phases with different parameters, $\Delta\zeta = \zeta_\alpha - \zeta_\beta$ that represent the difference between the permeability of polymer α and β to the membrane. Inspection of Fig. 2 shows that these morphological changes indicate a wetting transition from complete wetting to partial wetting and complete dewetting of phase
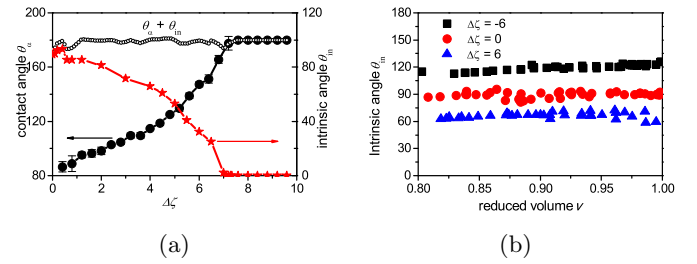

FIG. 3. (color online) (a) The effective contact angle θ_α and intrinsic contact angle θ_{in} obtained from the quasi-spherical vesicles ($v \approx 1.0$) as a function of $\Delta\zeta$, (b) The intrinsic angle θ_{in} as a function of the reduced volume v at varying $\Delta\zeta$.

α along with the increasing parameter $\Delta\zeta$. The material parameter, ζ_p, represents the impermeability of the membrane to the polymer, and Fig. 2 confirms that a polymer with larger ζ_p tends to remain in the interior of the vesicle. The three effective contact angles θ_α, θ_β and θ_γ in Fig. 1 obey the relation $\theta_\alpha + \theta_\beta + \theta_\gamma = 2\pi$, with regard to the three tensions $\Sigma_{\alpha\beta}$, $\Sigma_{\alpha\gamma}$, $\Sigma_{\beta\gamma}$ via the classical Neumann equations for the force balance at the junction point of three contact lines[4]. The proposed intrinsic contact angle θ_{in} has been defined in a previous report[13] as

$$\cos\theta_{in} = \frac{\sin\theta_\beta - \sin\theta_\alpha}{\sin\theta_\gamma} = \frac{\Sigma_{\alpha\gamma} - \Sigma_{\beta\gamma}}{\Sigma_{\alpha\beta}}. \quad (15)$$

However, in the quasi-spherical vesicles, $v \approx 1.0$, the effective contact angle θ_γ is close to 180^0, and thus the intrinsic contact angle θ_{in} can be estimated by the effective contact angle θ_β. Meanwhile, as presented in Ref. 13, the value of the intrinsic contact angles θ_{in} can also be determined from the geometrical relation

$$\theta_{in} = \psi(s) - \theta \quad (16)$$

where $\psi(s)$ is the local tilt angle at the $\alpha\beta$ interface, and θ is the tangent angle indicated in Fig. 1(b). From these morphologies, the intrinsic contact angle θ_{in} can be calculated via the geometrical relation. The resulting values for θ_α and θ_{in} are presented in Fig. 3(a) as a function of $\Delta\zeta$. As described in Fig. 3(a), the effective contact angle θ_α gradually increases up to 180^0 upon the increase of $\Delta\zeta$ from 0.0 to 7.0, while the intrinsic contact angle θ_{in} decreases. Likewise, we find that $\theta_\alpha + \theta_{in} \approx 180^0$, and thus $\theta_{in} \simeq \theta_\beta$ in these quasi-spherical vesicles. To further address the relation between the material parameter ζ_p and intrinsic contact angle θ_{in}, we studied a series of prolate vesicles containing α and β phases $(0.8 < v < 1.0)$ at three different material parameters $\Delta\zeta = -6.0$, 0.0 and 6.0 with a volume fraction of $\phi_\alpha/\phi_\beta = 0.3/0.7$, respectively. In previous publications[13,17], vesicles encapsulating two aqueous-aqueous phases usually take prolate shapes in a wide range of the reduced volume v from 1.0 to 0.8. Figure 3(b) gives the values for θ_{in} obtained

from the geometrical relation as a function of the reduced volume v. The intrinsic contact angle is found to be independent of the reduced volume v and to be roughly constant with $\theta_{in} = 119.69 \pm 3.46$ degrees at $\Delta\zeta = -6.0$, $\theta_{in} = 89.31 \pm 3.14$ degrees at $\Delta\zeta = 0.0$ and $\theta_{in} = 66.60 \pm 5.57$ degrees at $\Delta\zeta = 6.0$, respectively. Therefore, we claim that the intrinsic contact angle θ_{in} depends on the material parameter $\Delta\zeta$, but is independent of the geometric parameter, such as the reduced volume v.
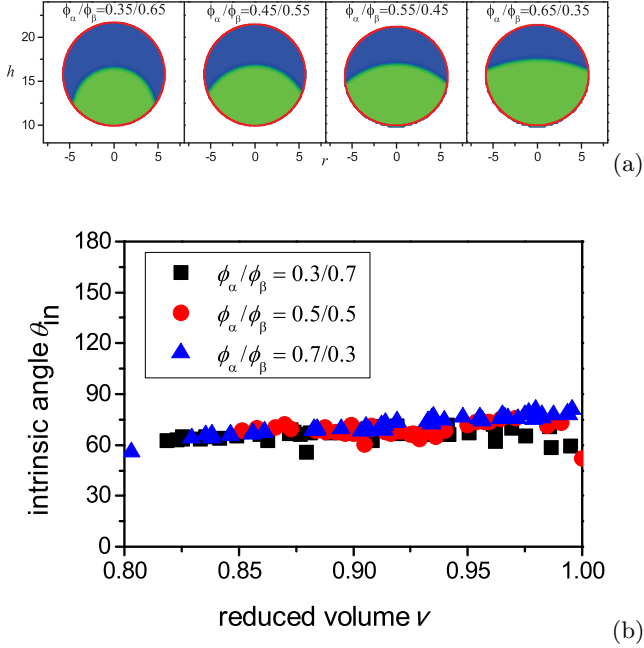

FIG. 4. (color online) (a) Phases of vesicles encapsulating phase α (green) and phase β (blue) with different volume fractions of ϕ_α/ϕ_β at $c_0 = 0$, $v \approx 1$, $\chi_{\alpha\beta} = 0.035$ and $\Delta\zeta = 6.0$, (b) The intrinsic angle θ_{in} as a function of the reduced volume v with different parameters ϕ_α/ϕ_β at $\Delta\zeta = 6$.

Fig. 4(a) shows that phase α (green) in these quasi-spherical vesicles occupies much more volume along with an increase in ϕ_α/ϕ_β that is not a material property. Additionally, the junction point between α, β and membrane moves toward the north pole of the spherical vesicle. However, it is found unexpectedly that the intrinsic angles obtained from the geometrical relation, Eq. (16), remain roughly constant close to $\theta_{in} = 65.37^0 \pm 5.5$. Likewise, the intrinsic contact angles are presented in Fig. 4(b) as a function of the reduced volume, $0.8 < v < 1.0$, at different volume fractions, ϕ_α/ϕ_β. The intrinsic contact angle is found to be independent of not only the reduced volume v but also the volume fraction of α and β, giving that $\theta_{in} \simeq 69.0^0 \pm 5.1$. Here, Flory Huggins interaction parameter, $\chi_{\alpha\beta}$, is chosen as 0.035, and the system is located in the deep quench regime. Flory-Huggins interaction parameter is expected to be linearly with the inverse temperature of the system, and depends on Hildebrand solubility parameter, the concentration and molec-
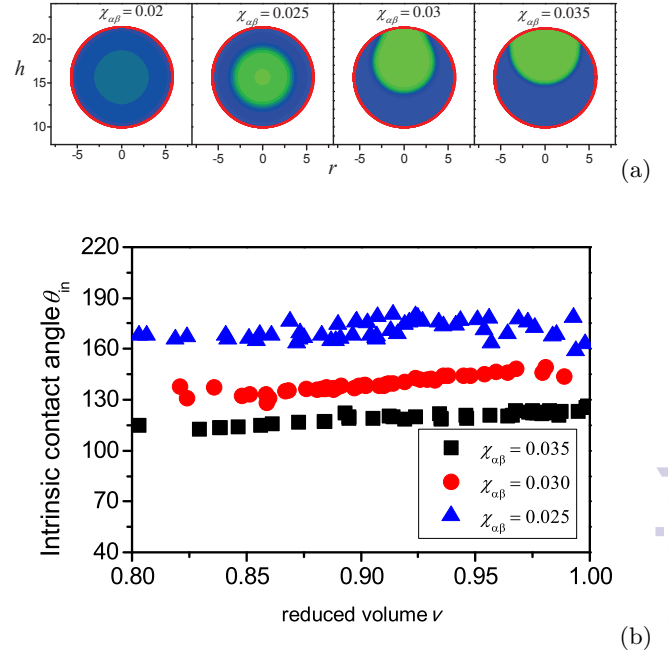

FIG. 5. (color online) (a) Phases of vesicles encapsulating phase α (green) and phase β (blue) with different Flory Huggins parameters, $\chi_{\alpha\beta}$ at $c_0 = 0$, $v \approx 1$, $\phi_\alpha/\phi_\beta = 0.3/0.7$ and $\Delta\zeta = 6.0$, (b) The intrinsic angle θ_{in} as a function of the reduced volume v with different parameters ϕ_α/ϕ_β at $\Delta\zeta = -6.0$.

ular weight of polymers[26]. Whereas, Self consistent field theory for polymers is confirmed to be effective when the system at the χ is located in the unstable region and far way from the critical point (in the deep quench regime)[27]. After thermodynamic equilibrium in the deep quench regime, the volume fraction reaches approximately to 1.0 in each phase. Indeed, the equilibrium compositions in phase α/β and interface width between phase α and β would be altered along with the decrease of $\chi_{\alpha\beta}$ to the binodal curve, where the system is close to the critical point (in the shallow quench regime)[28]. Accordingly, the values of $\zeta_\alpha\phi_\alpha$ and $\zeta_\beta\phi_\beta$ on the membrane are expected to depend on the Flory-Huggins interaction parameter close to the critical point (in the shallow quench regime). Fig. 5(a) presents the morphologies of a spherical vesicle containing two phases at different Flory-Huggins interaction parameters, $\chi_{\alpha\beta}$. It is found in the morphologies that phase α (green) also undergos the transition from complete dewetting to partial wetting along with an increase in $\chi_{\alpha\beta}$. When $\chi_{\alpha\beta}$ increases from 0.02 to 0.035 at $\phi_\alpha/\phi_\beta = 0.3/0.7$, the thermodynamic state of phase separation would be changed and the polymer blends may undergo the metastable and unstable region of the phase diagram[28]. At the metastable region, droplet starts to form and coarsens during the nucleation and growth process. At the unstable region, the clusters rapidly grow and coalesce until a single macroscopic phase forms. The intrinsic angle θ_{in} is also presented in Fig. 5(b) as a

function of reduced volume, v, at three $\chi_{\alpha\beta}$. θ_{in} is found to be independent of reduced volume, but dependent of $\chi_{\alpha\beta}$, giving that $\theta_{in} = 119.69 \pm 3.46$ degrees at $\chi_{\alpha\beta} = 0.035$, $\theta_{in} = 139.13 \pm 4.68$ degrees at $\chi_{\alpha\beta} = 0.03$ and $\theta_{in} = 170.64 \pm 5.32$ degrees at $\chi_{\alpha\beta} = 0.025$, respectively. With an change of $\chi_{\alpha\beta}$ in the shallow quench regime, both the interface energy between α and β, and polymer compositions at two phases would be altered, as well as the values of $\zeta_p\phi_p$ on the membrane. Therefore, the three tensions and the intrinsic contact angle θ_{in} would be changed so as to arrive at the force balance along with three contact lines.

In the experiment[5], transitions from complete to partial wetting were observed with membrane compartments as the external osmolarity increases. In order to obtain vesicles containing two phases, the polymer concentration is raised above binodal curve by the increase of the the external osmolarity (deflations) and phase separation occurs in the vesicle. With further increase of the external osmolarity, the polymer concentration would be raised above spinodal curve and enter into the unstable regime. Thus, the quench depth of phase separation is expected to be changed together with the increase of external osmolarity. As mentioned above, the quench depth of phase separation is also to be changed along with the Flory Huggins interaction parameter. Therefore, such wetting transitions dependent of the Flory Huggins interaction parameter that are identified in the calculations, are in well consistent with those observed experimentally[5].

In the presence of interactions between the membrane and polymer, the polymer in the interior of a vesicle not only leads to an extra pressure on the membrane, but also changes the local tension of the membrane, see Eq. 14. Likewise, in order to reduce the interaction energy between membrane and polymer, the configuration of polymer is altered as well. Inspection of Fig. 6(a) shows that the interface between phase α (green) and membrane is found to be increased along with the decrease of the parameter $\Delta\eta = \eta_{\alpha m} - \eta_{\beta m}$. The effective contact angle θ_α, however, is found to decrease from 121.62^0 at $\Delta\eta = 0$ to 1.01^0 at $\Delta\eta = -0.06$. Meanwhile, Fig. 6 (b) shows that θ_{in} still remains roughly constant regardless of the reduced volume, but the mean value of θ_{in} with regard to the reduced volumes shifts from $\theta_{in} \simeq 66.90 \pm 7.45$ degrees at $\Delta\eta = 0$ to $\theta_{in} \simeq 100.97 \pm 5.69$ degrees at $\Delta\eta = -0.04$. As a result, θ_{in} depends on the interaction parameter between the membrane and polymer, η, as a material parameter. In addition, the interfacial tensions have been proposed to be associated with the interactions between the lipid head groups and the two polymer phases.

IV. SUMMARY AND OUTLOOK

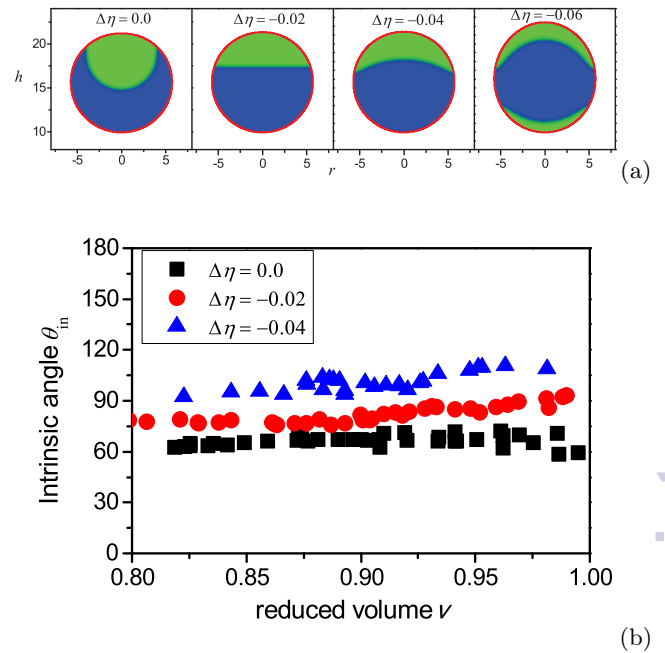For the membrane/polymer systems studied in Ref. 12 and 13, the proposed intrinsic contact angle θ_{in} repre-

FIG. 6. (color online) (a) Phase of vesicles encapsulating phase α (green) and phase β (blue) with different interactive parameters $\Delta\eta$ at $\phi_\alpha/\phi_\beta = 0.3/0.7$, $c_0 = 0$, $v \approx 1$, $\chi_{\alpha\beta} = 0.035$ and $\Delta\zeta = 6.0$, (b) The intrinsic angle θ_{in} as a function of the reduced volume v with different parameters $\Delta\eta$ at $\Delta\zeta = 6$.

sents 'a hidden variable', and is an essential property of the system. The wetting transitions within membrane compartments relevant to the intrinsic contact angle θ_{in} are associated with Flory Huggins interaction paramter $(\chi_{\alpha\beta})$ **close to the critical point**, the permeability of the membrane with respect to the polymer (ζ_p) and the interaction between the membrane and polymer (η_{pm}). For suitable concentrations of polymer α and β, this system of two aqueous phases may shift from one phase to the metastable phase that is between the binodal and spinodal curve, and then from metastable to unstable phase that is above spinodal curve along with the change of the temperature. Likewise, for suitable temperature, the concentrations of polymer α and β within membrane compartments is also expected to be raised above binodal curve by the increase of the external osmolarity (deflations) and phase separation occurs in the vesicle. In the experiment[5], the two aqueous phase system shifts from homogeneous phase to two phases by the increase external osmolarity, thereby undergoing metastable and unstable phases. Close to the critical point, the compositions of phase α and β are to be changed together with the quench depth of phase separation, thereby giving that the formation of phases α/β within a vesicle influences the vesicle shape via an inhomogeneous pressure and tension, as well as an intrinsic contact angle. Therefore, the wetting transitions within a vesicle that are identified along with the Flory Huggins interaction parameter agree with wetting transitions observed experimentally by the

increase of the external osmolarity (deflations)[5,6]. In particular, for a given ζ_p and η_p, that is a material property, the angle θ_{in} is found to be constant and independent of parameters that are not material properties, such as the reduced volume and volume fraction of phase α and β, in which is in consistent with the theoretical result presented in Ref. 13.

In the theoretical framework, the parameters ζ_p, η_{pm} and $\chi_{\alpha\beta}$ are introduced to describe the permeability of the membrane to polymers, interactions between polymers and the membrane and between polymer α and β, in which they are associated with different encapsulated polymers, e.g. different chain segments and molecular weight of polymers, and temperature, because different polymers would possess different permeability to the membrane and interactions between the polymer and the membrane and between polymers. The theoretical results presented here would provide guidance to future studies that are focused on the wetting transition within membrane compartments, including spherical vesicles, prolates, oblates and stomacytes. In future research, it is of great interest to extend the theoretical framework described here to study the phase behavior of vesicles induced by or modified by other complicated phases under membrane confinement.

[1] M. R. Moldover, J. W. Cahn Science **207**, 1073 (1980).

[2] D. Reinelt, V. Iov, P. Leiderer, J. Klier J. Phys. Condens. Matter **17**, S403(2005).

[3] D. Bonn, E. Bertrand, J. Meunier Phys. Rev. Lett. **84**, 4661(2000).

[4] J. S. Rowlinson and B. Widom, Molecular theory of capillarity (Clarendon Press. Oxford, 1989).

[5] Y. Li, R. Lipowsky, R. Dimova J. Am. Chem. Soc. **130**, 12252 (2008).

[6] N. Biswas, M. Ichikawa, K. Yoshikawa Chem. Phys. Lett. **539**, 157 (2012).

[7] B. Alberts et al., Molecular Biology of the cell (Garland Science, New York, 2002), 4th ed.

[8] Microcompartmentation and Phase Separation in Cytoplasm; Walter, H., Brooks, D. E., Srere, P. A.; Eds.; International Review of Cytology; Academic Press: San Diego, 2000; Vol. 192.

[9] M. S. Long, C. D. Jone, M. R. Helfrich, C. Keating Proc. Natl. Acad. Sci. USA **102**(17), 5920 (2005).

[10] M. S. Long, A. S. Cans, C. D. Keating J. Am. Chem. Soc. **130**(2), 756 (2008).

[11] M. A. Koback, C. D. Keating J. Am. Chem. Soc. J. Am. Chem. Soc. **133**(24), 9545 (2011).

[12] Y. H. Li, R. Lipowsky, R. Dimova Proc. Natl. Acad. Sci. USA **108**(12), 4731 (2011).

[13] H. Kusumaatmaja, Y. H. Li, R. Dimova, R. Lipowsky Phys. Rev. Lett. **103**(23), 238103 (2009).

[14] J. F. Wang, K. K. Guo, Y. L. Yang Phys. Rev. E **71**, 041908 (2005).

[15] K. K. Guo, F. Qiu J. Chem. Phys. **123**, 074906 (2005).

[16] K. K. Guo, F. Qiu, Y. L. Yang Soft Matter **5**, 1646 (2009).

[17] W. J. Xiao, K. K. Guo Soft Matter, **10**, 2539 (2014).

[18] W. Helfrich, Z. Naturforsch C **28**, 693 (1973).

[19] Z. C. Ou-Yang, W. Helfrich, Phys. Rev. Lett. **59**, 2486 (1989).

[20] F. Drolet, G. H. Fredrickson, Phys. Rev. Lett. **83**, 4317 (1999).

[21] U. Seifert, K. Berndl, R. Lipowsky, Phys. Rev. A **44**, 1182 (1991).

[22] R. Bar-Ziv, E. Moses Phys. Rev. Lett. **73**, 1392 (1994).

[23] N. Gov, A. G. Zilman, S. Safran, Phys. Rev. Lett. **90**, 228101 (2003).

[24] J. M. Nitsche, G. B. Kasting, J. Pharm. Sciences **102**(6), 2005 (2013).

[25] R. I. Sha Afi, C. M. Gary-Bobo, A. K. Solomon J. Gen. Physiology, **58**, 238 (1971).

[26] A. Eliassi, H. Modarress, J. Chem. Eng. Data **44**, 52 (1999).

[27] M. W. Matsen, J. Phys. Cond. Matter **14**(2) S0953 (2002).

[28] F. S. Bates, Science **251** 898 (1991).